Progress In Electromagnetics Research B, Vol. 17, 309–326, 2009

EM FIELD COUPLING TO NON-UNIFORM MICROSTRIP LINES USING COUPLED MULTI-CONDUCTOR STRIPS MODEL

H. Khodabakhshi and A. Cheldavi

College of Electrical Engineering
Iran University of Science and Technology
Tehran, Iran

Abstract—A model for the two-dimensional analysis of microstrip lines, named Rigorously Coupled Multi-conductor Strip (RCMS) is introduced. In this model, the width of the strip of a microstrip line is subdivided into a large number of rigorously coupled narrow strips. So, a microstrip line can be considered as a coupled multi-conductor transmission line. Determination of the capacitance and inductance matrices of the model is introduced, also. The voltages and currents induced by electromagnetic fields for the coupled multi-condutor strips problem can be obtained using Bernardi's method. The effect of an external EM wave on a microstrip line with non-uniformity in its width is computed by adding the circuit model of transverse discontinuity (narrow slit) to the RCMS model. Finally, the validity and efficiency of the introduced method is investigated using previous work and full wave EM-simulation software.

1. INTRODUCTION

Microstrip transmission lines are widely used in microwave and millimeter wave circuits and systems. There are several classical methods for the analysis of such structures in the literature. Almost all of these methods can be categorized into two methods, the transmission line method [1, 2] and full-wave analysis [3, 4]. The transmission line method is a simple model that cannot consider the current distribution in the width of the strip, because the whole width of the strip is considered as one line. To consider the non-uniformity of the current along the width of the strip, full-wave analysis has to be used, which is sometimes difficult and time-consuming.

Corresponding author: H. Khodabakhshi (khodabakhshi.hamid@gmail.com).

In this paper, a simple rigorously coupled multi-conductor strips model (RCMS) is used to find the voltage and current induced by an external electromagnetic field. In this method, a microstrip line with a wide strip is modeled by a very large number of parallel microstrip lines with narrow strips, as shown in Fig. 1(a). The air gap between these narrow strips is very small and their total width is equal to the width of the main strip. All the elementary strips are connected together and a single load is set at each termination. This model is good if one considers only longitudinal current on the strips (quasi-TEM approximation). Also, Fig. 1(b) shows the RCMS model of terminal conditions. Fig. 2 shows two types of such non-uniformities, a grounded via and a transverse slit. To investigate the effect of an external EM field on a non-uniform microstrip line, we simply add the circuit model of the discontinuity to RCMS model.

First the capacitance and inductance matrices needed for the RCMS method have been extracted in Section 2. The effect of an external electromagnetic field on coupled transmission lines has been investigated using Bernardi's method, in Section 3. The forced terms due to incident wave are then obtained, in Section 4. The induced voltage and current along the uniform and non-uniform line is evaluated using the RCMS model and modal decoupling method, in Section 5. Finally, microstrip line structures with uniformity and non-uniformity (transverse slit) in their width have been analyzed based on the RCMS model and the validity and efficiency of the introduced method has been verified by previous work and full wave EM-simulation (HFSS).

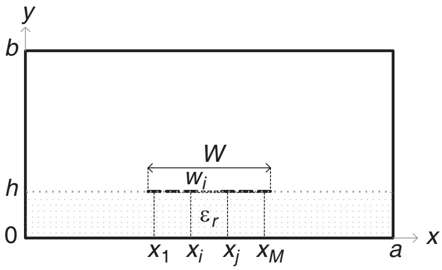

(a)

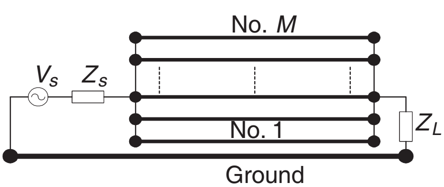

(b)

Figure 1. (a) The cross section of M rigorously coupled microstrip lines with width of $w = W/M$ (the RCMS model). (b) The terminal conditions of the RCMS model.

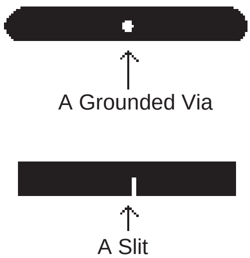

Figure 2. Two types of transverse non-uniformities in a microstrip, a grounded via and a transverse slit.

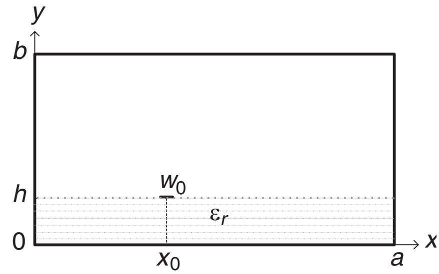

Figure 3. The cross section of the structure used for extracting the capacitance matrix of the microstrip line shown in Fig. 1.

2. DETERMINATION OF C AND L MATRICES

To use the RCMS model, one needs to find its **C** and **L** matrices. There are some methods to derive **C** and **L** matrices in the literature [5, 6]. In this section a simple method is introduced to obtain the capacitance matrix **C**. The capacitance matrix can be obtained using the two-dimensional analysis of the shielded structure as shown in Fig. 1(a).

The dimensions of the shielding box must be carefully selected, so that the metal shield does not perturb the field lines localized around the narrow strips. So, the conditions of $a \geq (10h + W)$ and $b \geq 10h$ must be satisfied.

The inductance matrix **L** can be obtained using the following simple relation:

$$\mathbf{L} = \frac{1}{c^2}\mathbf{C}_0^{-1}. \tag{1}$$

where $\mathbf{C}_0$ is the capacitance matrix for $\varepsilon_r = 1$. In order to obtain the capacitance matrix **C**, first we consider a charge Q distributed uniformly in a very narrow width, w_0, on the boundary $y = h$, as shown in Fig. 3.

Solving the two dimensional Laplace's equation with boundary conditions $V(x, 0) = V(x, b) = V(0, y) = V(a, y) = 0$ and the continuity of voltage on the $y = h$, the voltage distribution is obtained as follows:

$$V(x,y) = \begin{cases} V_1(x,y) = \sum\limits_{n=1}^{\infty} A_n \sin\left(\frac{n\pi}{a}x\right) \frac{\sinh\left(\frac{n\pi}{a}y\right)}{\sinh\left(\frac{n\pi}{a}h\right)}; & 0 \leq y \leq h \\ V_2(x,y) = \sum\limits_{n=1}^{\infty} A_n \sin\left(\frac{n\pi}{a}x\right) \frac{\sinh\left(\frac{n\pi}{a}(b-y)\right)}{\sinh\left(\frac{n\pi}{a}(b-h)\right)}; & h \leq y \leq b \end{cases}. \tag{2}$$

Using (2), the surface charge on the $y = h$ boundary is obtained as

$$\rho_s(x,h) = \varepsilon_0 \left(\varepsilon_r \frac{\partial V_1}{\partial y}\Big|_{y=h} - \frac{\partial V_2}{\partial y}\Big|_{y=h} \right) = \sum_{n=1}^{\infty} B_n A_n \sin\left(\frac{n\pi}{a} x\right). \quad (3)$$

in which

$$B_n = \varepsilon_0 \frac{n\pi}{a} \left[\varepsilon_r \coth\left(\frac{n\pi}{a} h\right) + \coth\left(\frac{n\pi}{a}(b-h)\right) \right]. \quad (4)$$

It is assumed that the surface charge distribution on the $y = h$ boundary is zero except in a very narrow region $x_0 - w_0/2 < x < x_0 + w_0/2$, shown in Fig. 3, in which it is equal to a constant value Q/w_0. Then using (3) the unknown coefficients A_n are obtained as

$$A_n = \frac{4}{n\pi B_n w_0} \frac{Q}{w_0} \sin\left(n\pi \frac{x_0}{a}\right) \sin\left(n\pi \frac{w_0}{2a}\right). \quad (5)$$

Using (5) in (2), the voltage on the boundary $y = h$ becomes

$$V(x,h) = \frac{4}{\pi w_0} Q \sum_{n=1}^{\infty} \frac{1}{n B_n} \sin\left(n\pi \frac{x}{a}\right) \sin\left(n\pi \frac{x_0}{a}\right) \sin\left(n\pi \frac{w_0}{2a}\right). \quad (6)$$

Now, the voltage of the j-th strip shown in Fig. 1(a) due to the charge Q_i on the i-th strip can be written as follows

$$\begin{aligned} V_j &= \frac{4}{\pi w_0} Q_i \sum_{n=1}^{\infty} \frac{1}{n B_n} \sin\left(n\pi \frac{x_j}{a}\right) \sin\left(n\pi \frac{x_i}{a}\right) \sin\left(n\pi \frac{w_0}{2a}\right); \\ x_i &= \left(\frac{a-W}{2}\right) + (2i-1)\frac{w_0}{2} + (i-1)s \\ x_j &= \left(\frac{a-W}{2}\right) + (2j-1)\frac{w_0}{2} + (j-1)s, \quad i,j = 1,2,\ldots,M. \end{aligned} \quad (7)$$

where s is the width of the gaps between narrow strips.

If the number of unknown coefficients is truncated by $n \leq N$, the relations in (7) can be written in a matrix form, as follows

$$\mathbf{V}_{M\times 1} = \mathbf{P}_{M\times M} \mathbf{Q}_{M\times 1}. \quad (8)$$

in which each element of the matrix $\mathbf{P}$, i.e., $\mathbf{P}(j,i)$, is obtained using the summation of N terms. So, the capacitance matrix is obtained, as

$$\mathbf{Q}_{M\times 1} = \mathbf{C}_{M\times M} \mathbf{V}_{M\times 1}, \quad \mathbf{C} = \mathbf{P}^{-1}. \quad (9)$$

The number N must be carefully selected so that the N-th term of the summation in (7) can be considered much smaller than its first term. So, using (7) and (4), for the worst case one has

$$N \gg \sqrt{\frac{\varepsilon_r \coth(\frac{\pi}{a}h)+1}{\varepsilon_r+1}\frac{1}{\sin(\pi\frac{w}{2a})\sin^2(\pi\frac{x_1}{a})}}. \tag{10}$$

3. EFFECT OF AN EXTERNAL EM FIELD ON THE COUPLED TRANSMISSION LINES

The structure of uniform coupled microstrip lines is depicted in Fig. 4, where it is illuminated by a uniform plane wave. To determine the disturbance induced in the coupled transmission lines, we follow the procedure proposed in [9, 11].

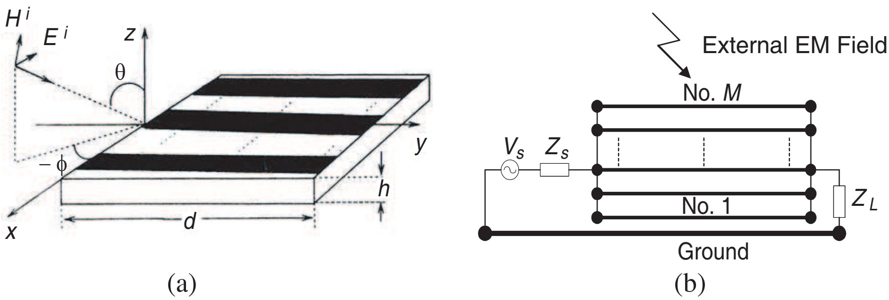

Figure 4. RCMS model for a microstrip line excited by the external field.

Considering the equation $\nabla \times \vec{E} = -j\omega\mu_0\vec{H}$ and integrating over the rectangular area enclosed by the path 1–4 shown in Fig. 5, and using Stokes' theorem, we obtain [9]

$$-\frac{d}{dy}\int_0^h E_z(x_k, y, z)dz = j\omega\mu_0\int_0^h H_x(x_k, y, z)dz. \tag{11}$$

Consider now the continuity equation $\nabla \cdot (\vec{J} + j\omega\varepsilon_r\vec{E}) = 0$. Integrate this equation over the elementary volume containing the k-th strip (Fig. 6) and apply the divergence theorem [9]

$$\begin{aligned}\frac{d}{dy}\int_{x_k-\frac{w_k}{2}}^{x_k+\frac{w_k}{2}} \vec{J}_s(x,y)\cdot\hat{y}dx =& j\omega\int_{x_k-\frac{w_k}{2}}^{x_k+\frac{w_k}{2}} \varepsilon_0\varepsilon_r E_z(x,y,h^-)dx \\ &-j\omega\int_{x_k-\frac{w_k}{2}}^{x_k+\frac{w_k}{2}} \varepsilon_0 E_z(x,y,h^+)dx.\end{aligned} \tag{12}$$

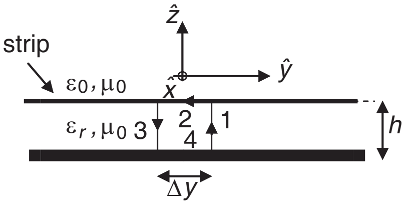

Figure 5. Path of integration in y-z plane.

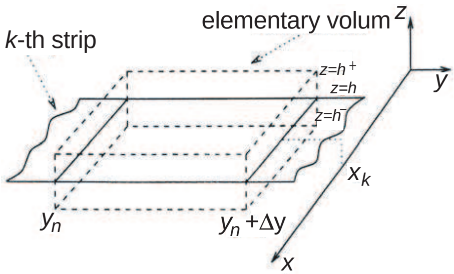

Figure 6. Elementary volume containing the k-th strip.

where $\vec{J}_s$ is the surface current on the strip excited by the external field.

Let us define the following quantities:

Induced voltage of k-th strip

$$V_k(y) = -\int_0^h E_z(x_k, y, z)dz. \tag{13}$$

Induced current of k-th strip

$$I_k(y) = \int_{x_k-\frac{w_k}{2}}^{x_k+\frac{w_k}{2}} \vec{J}_s(x, y) \cdot \hat{y}dx. \tag{14}$$

Electric charge per unit length of k-th strip

$$Q_k(y) = \int\limits_{x_k-\frac{w_k}{2}}^{x_k+\frac{w_k}{2}} \varepsilon_0 E_z(x, y, h^+) - \varepsilon_0\varepsilon_r E_z(x, y, h^-)dx. \tag{15}$$

Magnetic flux per unit length of k-th strip

$$\Phi_k(y) = -\int_0^h \mu_0 H_x(x_k, y, z)dz. \tag{16}$$

With these definitions, (11) and (12) become

$$\frac{d}{dy}V_k(y) = -j\omega\mu_0\Phi_k(y) \tag{17}$$

$$\frac{d}{dy}I_k(y) = -j\omega Q_k(y). \tag{18}$$

We decompose the total field into a sum of a primary and a secondary field. The primary field is defined as the field excited by the incident wave in the presence of the ground plane and the dielectric substrate, and in the absence of the metal strips. The secondary field is the field scattered by the strips in the presence of the ground plane and the dielectric substrate [9]:

$$\begin{aligned} E(x, y, z) &= E^p(x, y, z) + E^s(x, y, z) \\ H(x, y, z) &= H^p(x, y, z) + H^s(x, y, z). \end{aligned} \tag{19}$$

Substituting (19) into (15) and (16), (17) and (18) become

$$\frac{d}{dy} V_k(y) = -j\omega\Phi_k^p(y) - j\omega\Phi_k^s(y) \tag{20}$$

$$\frac{d}{dy} I_k(y) = -j\omega Q_k^s(y). \tag{21}$$

where

$$\Phi_k^j(y) = -\int_0^h \mu_0 H_x^j(x_k, y, z)dz \quad j = p, s \tag{22}$$

$$Q_k^j(y) = \int\limits_{x_k-\frac{w}{2}}^{x_k+\frac{w}{2}} \varepsilon_0 E_z^j(x, y, h^+) - \varepsilon_0\varepsilon_r E_z^j(x, y, h^-)dx. \tag{23}$$

Suppose that the incident field only excites the quasi-TEM dominant mode in this structure. So, we have

$$\Phi_k^s(y) = [L_{k1}, L_{k2}, \ldots, L_{kM}][I_1(y), I_2(y), \ldots, I_M(y)]^t \qquad k = 1, 2, \ldots, M. \tag{24}$$

Substituting (24) into (20), a matrix differential equation can be obtained

$$\frac{d}{dy}[V] + j\omega[L][I] = [V_F]. \tag{25}$$

where

$$\begin{aligned} [V]^T &= [V_1(y)V_2(y), \ldots, V_M(y)] \\ [I]^T &= [I_1(y)I_2(y), \ldots, I_M(y)] \\ [V_F] &= j\omega\mu_0 \\ &\left[\int_0^h H_x^p(x_1, y, z)dz, \int_0^h H_x^p(x_2, y, z)dz, \ldots, \int_0^h H_x^p(x_M, y, z)dz\right]^T \end{aligned} \tag{26}$$

and the $\mathbf{L}$ matrix can be obtained from Section 2.

Under the quasi-TEM mode excitation assumption, we have

$$Q_k^s(y) = [C_{k1}C_{k2}, \ldots, C_{kM}]\,[V^s]\,, \quad k = 1, 2, \ldots, M. \tag{27}$$

where

$$[V^s] = [V_1(y), V_2(y), \ldots, V_M(y)]^T - \left[V_1^p(y), V_2^p(y), \ldots, V_M^p(y)\right]^T \tag{28}$$

$$\begin{aligned} V_k^s(y) &= -\int\limits_0^h E_z^s(x_k, y, z)dz = V_k(y) - V_k^p(y) \\ &= \int_0^h E_z^p(x_k, y, z)dz - \int_0^h E_z(x_k, y, z)dz. \end{aligned} \tag{29}$$

Substituting (27) into (21), a matrix differential equation will be obtained

$$\frac{d}{dy}[I] + j\omega\ [C][V] = j\omega\ [C]\,[V^p] =\ [I_F]. \tag{30}$$

where

$$[I_F]=j\omega[C]\left[\int_0^h E_z^p(x_1, y, z)dz, \int_0^h E_z^p(x_2, y, z)dz, \ldots, \int_0^h E_z^p(x_M, y, z)dz\right]^T \tag{31}$$

and the $\mathbf{C}$ matrix can be obtained from Section 2.

In the next section, we evaluate the forced terms in (25) and (30) in terms of primary fields.

4. EVALUATION OF THE FORCED TERMS

To evaluate the forced terms in (25) and (30), we follow the same procedure as in [9]. Suppose that the incident wave is a uniform plane wave propagating in the $\hat{\beta}_i$ direction that forms an angle θ_i with z positive axis.

$$\begin{aligned} \vec{E}^i &= E_0 e^{-j\vec{\beta}^i \cdot \vec{r}} \\ \vec{H}^i &= \frac{\left(\hat{\beta}_i \times \vec{E}^i\right)}{\eta_0}. \end{aligned} \tag{32}$$

where $\vec{\beta}_i$ is the propagation vector and r the position vector.

The propagation vector can be decomposed into transverse and axial components with respect to the z direction [9]:

$$\vec{\beta}^i = \vec{\beta}_t + \beta_z \hat{z}. \tag{33}$$

We choose new orthogonal coordinates u, v with the v axis oriented in the β_t direction. So, the plane of incident is the v-z plane, and the field can be decomposed into the sum of TE and TM waves [9]:

$$\vec{\beta}_t = \beta_x \hat{x} + \beta_y \hat{y} = \beta_t \hat{v} = K_0 \sqrt{1 - \left(\hat{z} \cdot \hat{\beta}_i\right)^2} \hat{v}. \tag{34}$$

For the TE and TM waves, the transverse components of the electromagnetic field satisfy transmission line equations, where the wave impedances are [9]

$$\begin{aligned} Z_j^{TE} &= \frac{\omega \mu_0}{\beta_{zj}}, \quad (j = 1, 2) \\ Z_j^{TM} &= \frac{\beta_{zj}}{\omega \varepsilon_j} \end{aligned} \tag{35}$$

and the propagation constants

$$\beta_{zj} = K_0 \sqrt{(\varepsilon_{rj} - 1) + \left(\hat{z} \cdot \hat{\beta}_i\right)^2}. \tag{36}$$

In (35) and (36), the index $j = 1$ refers to substrate and $j = 2$ to the free space.

It is now possible to evaluate the forced terms

$$\begin{aligned} V_{Fk} &= -j 2 \omega \mu_0 \frac{\sin(\beta_{z_1} h)}{\beta_{z_1}} \\ &\quad \left\{ \frac{\vec{E}_0 \cdot \hat{v}}{j Z_1^{TM} \sin(\beta_{z_1} h) + Z_2^{TM} \cos(\beta_{z_1} h)} \, \hat{x} \cdot \hat{u} \right. \\ &\quad \left. + \frac{\vec{E}_0 \cdot \hat{u}}{j Z_1^{TE} \sin(\beta_{z_1} h) + Z_2^{TE} \cos(\beta_{z_1} h)} \hat{x} \cdot \hat{v} \right\} \cdot e^{-j\beta_x x_k - j\beta_y y} \qquad (37) \\ I_{Fk} &= j\omega \sum_{i=1}^{M} C_{ki} \left(\frac{-2\beta_t}{\omega \varepsilon_1} \right) . \frac{\sin(\beta_{z_1} h)}{\beta_{z_1}} \\ &\quad \left\{ \frac{\vec{E}_0 \cdot \hat{v}}{j Z_1^{TM} \sin(\beta_{z_1} h) + Z_2^{TM} \cos(\beta_{z_1} h)} \right\} e^{-j\beta_x x_i - j\beta_y y}, \\ &\qquad (k = 1, \ldots, M). \qquad (38) \end{aligned}$$

where C_{ki} is the ki-th element of $\mathbf{C}$ matrix.

5. EVALUATION OF THE INDUCED VOLTAGE AND CURRENT ALONG THE LINE

In this section, we solve the (25) and (30) using the modal decoupling method [8]. We assume that the principal propagation mode of the lines is TEM. This assumption is valid when the strip widths and their distances from the shield are small enough compared to the wavelength.

The differential equations describing M coupled transmission lines illuminated by a uniform plane wave are given by

$$\begin{aligned} \frac{d\mathbf{V}(y)}{dy} &= -\mathbf{Z}\,\mathbf{I}(y) + \mathbf{V}_F \\ \frac{d\mathbf{I}(y)}{dy} &= -\mathbf{Y}\,\mathbf{V}(y) + \mathbf{I}_F. \end{aligned} \tag{39}$$

in which $\mathbf{Z} = j\omega\mathbf{L}, \mathbf{Y} = j\omega\,\mathbf{C}$. y is the position along the lines, and V and I are voltage and current vectors, i.e., the voltages and currents of the lines in RCMS model, defined as

$$\begin{aligned} \mathbf{V}(y) &= [V_1(y) \ \ V_2(y) \ \ \ldots \ \ V_M(y)]^T \\ \mathbf{I}(y) &= [I_1(y) \ \ I_2(y) \ \ \ldots \ \ I_M(y)]^T. \end{aligned} \tag{40}$$

Also, $\mathbf{L}$ and $\mathbf{C}$ in (39) are inductance and capacitance matrices, respectively introduced in Section 2.

The differential equations in (39) can be decoupled using the definition of modal voltage and current vectors as

$$\begin{aligned} \mathbf{V}^m(y) &= \mathbf{T}_V^{-1}\mathbf{V}(y) \\ \mathbf{I}^m(y) &= \mathbf{T}_I^{-1}\mathbf{I}(y). \end{aligned} \tag{41}$$

where T_V and T_I are transfer or mode matrices determined from inductance and capacitance matrices [5]. Setting (41) in (39), the decoupled equations are obtained as

$$\begin{aligned} \frac{d\mathbf{V}^m(y)}{dy} &= -j\omega\mathbf{L}^m\mathbf{I}^m(y) + \mathbf{T}_V^{-1}\mathbf{V}_F(y) \\ \frac{d\mathbf{I}^m(y)}{dy} &= -j\omega\mathbf{C}^m\mathbf{V}^m(y) + \mathbf{T}_I^{-1}\mathbf{I}_F(y). \end{aligned} \tag{42}$$

in which $\mathbf{L}^m$ and $\mathbf{C}^m$ are diagonal inductance and capacitance matrices derived from the following matrix Equations [5]:

$$\mathbf{T}_V^{-1}\mathbf{L}\mathbf{T}_I = \mathbf{L}^m, \quad \mathbf{T}_I^{-1}\mathbf{C}\mathbf{T}_V = \mathbf{C}^m. \tag{43}$$

Now, we consider two cases of uniform and non-uniform microstrip lines:

5.1. Uniform Microstrip Line

In this case, the microstrip line has no non-uniformity in its width and (42) can be solved as [11]

$$\begin{aligned} \mathbf{I}(y) &= \mathbf{T}_I(\mathbf{e}^{-\gamma y}\mathbf{I}^{m+} - \mathbf{e}^{+\gamma y}\mathbf{I}^{m-}) + \mathbf{I}_{Fm}(y) \\ \mathbf{V}(y) &= \mathbf{Z}_C\mathbf{T}_I(\mathbf{e}^{-\gamma y}\mathbf{I}^{m+} + \mathbf{e}^{+\gamma y}\mathbf{I}^{m-}) + \mathbf{V}_{Fm}(y). \end{aligned} \tag{44}$$

where

$$\begin{aligned} \mathbf{I}_{Fm}(y) &= \left(\left[\boldsymbol{\beta}_y^2\right]_d + \left[\boldsymbol{\gamma}^2\right]_d\right)^{-1}\left(j\beta_y\left[\mathbf{I}_F\right] + \left[\mathbf{Y}\right]\left[\mathbf{V}_F\right]\right) \\ \mathbf{V}_{Fm}(y) &= j\beta_y\left[\mathbf{Y}\right]^{-1}\left(\left[\boldsymbol{\beta}_y^2\right]_d + \left[\boldsymbol{\gamma}^2\right]_d\right)^{-1} \\ &\qquad \left(j\beta_y\left[\mathbf{I}_F\right] + \left[\mathbf{Y}\right]\left[\mathbf{V}_F\right]\right) + \left[\mathbf{Y}\right]^{-1}\left[\mathbf{I}_F\right]. \end{aligned} \tag{45}$$

in which $\mathbf{I}^{m+}$ and $\mathbf{I}^{m-}$ are two constant vectors. $\left[\boldsymbol{\beta}_y^2\right]_d$, $\left[\boldsymbol{\gamma}^2\right]_d$ are diagonal matrices, β_y is phase constant of incident wave, and

$$\begin{aligned} \gamma^2 &= \mathbf{T}_V^{-1}\mathbf{Z}\mathbf{Y}\mathbf{T}_V = \mathbf{T}_I^{-1}\mathbf{Y}\mathbf{Z}\mathbf{T}_I \\ &= -\omega^2\mathbf{L}_m\mathbf{C}_m = -\omega^2\mathbf{C}_m\mathbf{L}_m \\ \mathbf{Z}_C &= \mathbf{Y}^{-1}\mathbf{T}_I\gamma T_I^{-1} = \mathbf{Z}\mathbf{T}_I\gamma^{-1}\mathbf{T}_I^{-1}. \end{aligned} \tag{46}$$

Using the following terminal conditions ($V_s = 0$)

$$\mathbf{V}(0) = -\mathbf{Z}_s\mathbf{I}(0), \quad \mathbf{V}(d) = \mathbf{Z}_L\mathbf{I}(d). \tag{47}$$

And inserting $y = 0$ and $y = d$ in (44), one can determine the following matrix equation to find unknown constant vectors $\mathbf{I}^{m+}$ and $\mathbf{I}^{m-}$:

$$\begin{bmatrix} (\mathbf{Z}_c + \mathbf{Z}_s)\mathbf{T}_I & (\mathbf{Z}_c - \mathbf{Z}_s)\mathbf{T}_I \\ (\mathbf{Z}_c - \mathbf{Z}_L)\mathbf{T}_I\mathbf{e}^{-\gamma d} & (\mathbf{Z}_c + \mathbf{Z}_L)\mathbf{T}_I\mathbf{e}^{-\gamma d} \end{bmatrix}\begin{bmatrix} \mathbf{I}^{m+} \\ \mathbf{I}^{m-} \end{bmatrix} = \begin{bmatrix} -\mathbf{V}_{Fm}(0) - \mathbf{Z}_s\mathbf{I}_{Fm}(0) \\ -\mathbf{V}_{Fm}(d) + \mathbf{Z}_L\mathbf{I}_{Fm}(d) \end{bmatrix}. \tag{48}$$

Finding these two constant vectors leads us to find the voltage and current vectors using (44). In (47), $\mathbf{Z}_L$ and $\mathbf{Z}_S$ are the load and source impedance matrices, respectively. These matrices for the structure shown in Fig. 4 are as follows

$$\mathbf{Z}_s = Z_s\mathbf{1}_{M\times M}, \quad \mathbf{Z}_L = Z_L\mathbf{1}_{M\times M}, \quad \mathbf{V}_s = V_s\mathbf{1}_{M\times 1}. \tag{49}$$

in which $\mathbf{1}$ is a matrix or vector that all its elements are 1.

Once the voltage and current of each narrow strip are obtained, the voltage $V(y)$, and current $I(y)$ microstrip line can be obtained as

$$V(y) = \frac{1}{M}\sum_{n=1}^{M} V_n(y), I(y) = \sum_{n=1}^{M} I_n(y). \tag{50}$$

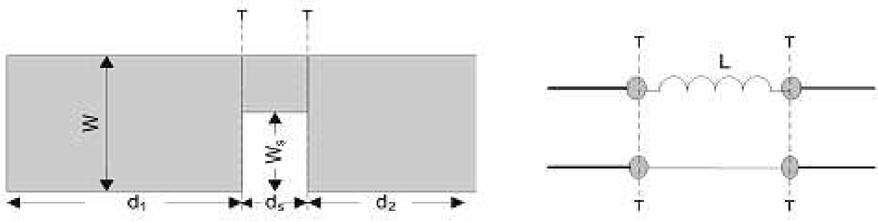

Figure 7. Model of the narrow transverse slit in a microstrip line.

5.2. Non-uniform Microstrip Line

To investigate the effect of an external EM field on a microstrip line with a non-uniformity in its width, we apply the RCMS model to the transverse discontinuity.

We consider a narrow transverse slit in a microstrip line. This leads to a local concentration of the magnetic field which can be described in terms of equivalent series inductivity [10]. Fig. 7 shows a microstrip of width W containing a slit of depth W_s and width d_s. The equivalent series inductance is obtained as [10]

$$\frac{L_s}{h} = \frac{\mu_0 \pi}{2}\left(1 - \frac{Z_0}{Z_0'}\right)^2 \left(\frac{H}{m}\right). \tag{51}$$

where Z_0 and Z_0' are the characteristic impedances of the air-filled uniform microstrip lines of width W and $W - W_s$, respectively.

Now, we solve the (43) for two segments of the line, i.e., $0 < y < d_1,\ d_1 + d_s < y < d$.

$$\begin{aligned} \mathbf{I}(y) &= \mathbf{T}_I(\mathbf{e}^{-\gamma y}\mathbf{I}_m^+ - \mathbf{e}^{+\gamma y}\mathbf{I}_m^-) + I_{Fm}(y); \quad 0 < y < d_1 \\ \mathbf{I}(y) &= \mathbf{T}_I(\mathbf{e}^{-\gamma y}\hat{\mathbf{I}}_m^+ - \mathbf{e}^{+\gamma y}\hat{\mathbf{I}}_m^-) + I_{Fm}(y); \quad d_1 + d_s < y < d. \end{aligned} \tag{52}$$

in which $\mathbf{I}_m^+$, $\mathbf{I}_m^-$, $\hat{\mathbf{I}}_m^+$ and $\hat{\mathbf{I}}_m^-$ are four unknown constant vectors. The voltage vector can be obtained in terms of current vector using (52) and (39).

In addition to the terminal conditions in (47), we have the following boundary conditions

$$\mathbf{V}(d_1 + d_s) - \mathbf{V}(d_1) = j\omega \mathbf{L}_{slit}\mathbf{I}(d_1), \quad \mathbf{I}(d_1 + d_s) = \mathbf{I}(d_1). \tag{53}$$

where $\mathbf{L}_{slit} = L_s \mathbf{1}_{M\times M}$. Using (47) and (53), one can determine the following matrix equation to find unknown constant vectors $\mathbf{I}_m^+$, $\mathbf{I}_m^-$,

$\hat{\mathbf{I}}_m^+$ and $\hat{\mathbf{I}}_m^-$:

$$\begin{pmatrix} (\mathbf{Z}_c+\mathbf{Z}_s)\mathbf{T}_I & (\mathbf{Z}_c-\mathbf{Z}_s)\mathbf{T}_I & 0 & 0 \\ 0 & 0 & (\mathbf{Z}_c-\mathbf{Z}_L)\mathbf{T}_I\mathbf{e}^{-\gamma d} & (\mathbf{Z}_c+\mathbf{Z}_L)\mathbf{T}_I\mathbf{e}^{\gamma d} \\ \mathbf{T}_I\mathbf{e}^{-\gamma d_1} & -\mathbf{T}_I\mathbf{e}^{\gamma d_1} & -\mathbf{T}_I\mathbf{e}^{-\gamma(d_1+d_s)} & \mathbf{T}_I\mathbf{e}^{\gamma(d_1+d_s)} \\ (\mathbf{Z}_{slit}+\mathbf{Z}_c)\mathbf{T}_I\mathbf{e}^{-\gamma d_1} & -(\mathbf{Z}_{slit}-\mathbf{Z}_c)\mathbf{T}_I\mathbf{e}^{\gamma d_1} & -\mathbf{Z}_c\mathbf{T}_I\mathbf{e}^{-\gamma(d_1+d_s)} & -\mathbf{Z}_c\mathbf{T}_I\mathbf{e}^{\gamma(d_1+d_s)} \end{pmatrix}$$
$$\begin{bmatrix} \mathbf{I}_m^+ \\ \mathbf{I}_m^- \\ \hat{\mathbf{I}}_m^+ \\ \hat{\mathbf{I}}_m^- \end{bmatrix} = \begin{bmatrix} -\mathbf{V}_{Fm}(0)-\mathbf{Z}_s\mathbf{I}_{Fm}(0) \\ -\mathbf{V}_{Fm}(d)+\mathbf{Z}_L\mathbf{I}_{Fm}(d) \\ \mathbf{I}_{Fm}(d_1+d_s)-\mathbf{I}_{Fm}(d_1) \\ \mathbf{V}_{Fm}(d_1+d_s)-\mathbf{V}_{Fm}(d_1)-\mathbf{Z}_{slit}\mathbf{I}_{Fm}(d_1) \end{bmatrix}. \tag{54}$$

where $\mathbf{Z}_{slit} = j\omega\mathbf{L}_{slit}$.

Finding these four constant vectors leads us to find the voltage and current vectors using (52) and (39).

Once the voltage and current of each narrow strip are obtained, the voltage $V(y)$, and current $I(y)$ microstrip line can be obtained using (50).

6. NUMERICAL RESULTS

In this section, two unshielded microstrip line structures using two-dimensional analysis have been analyzed based on the RCMS model. Consider the first microstrip line as shown in Fig. 1 with $W = 3.85$ mm, $h = 1.57$ mm, $\varepsilon_r = 2.55$, and $a = b = 100W$. The second structure is a microstrip line with a narrow transverse slit with $W = 3.85$ mm, $h = 1.57$ mm, $\varepsilon_r = 2.55$, $a = b = 100W$, and $d_1 = 6$ cm, $d_s = 0.785$ mm, and $W_s = W/2 = 1.925$ mm. Both lines are $d = 15$ cm long and are terminated in their characteristic impedance at both ends ($Z_o = 50$). Then consider the RCMS model as shown in Fig. 1 containing $M = 51$ narrow strips with the same width and with very small air gap between them. The incident field is a uniform plane wave with an electric field intensity of 1 V/m, whose plane of incidence is the x-z plane or the y-z plane and θ_i is the incidence angle with respect to z axis.

Figure 8 shows the voltage and current magnitude induced along the first line for $\theta_i = 0$ at frequency of 3 GHz. In both figures, it is seen that there is a good agreement between the results obtained using the method proposed in [9], the RCMS method and the HFSS. The amplitudes of the induced voltage and current are symmetric with respect to the center of line. So, the induced powers at terminal loads are equal.

To investigate the sensitivity of the number of the segments (M) and the width of the gap (s) to the overall performance, we present the effects of these parameters on the current distribution excited in

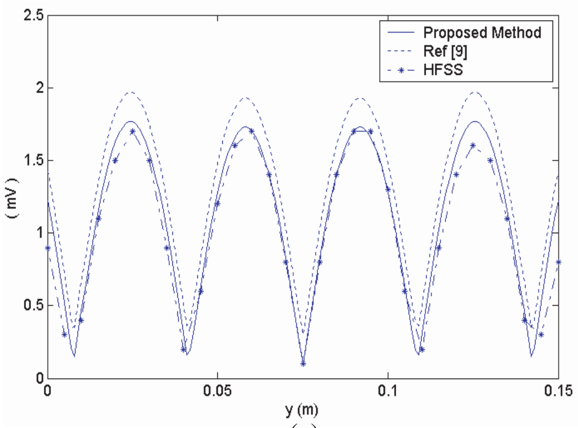

(a)

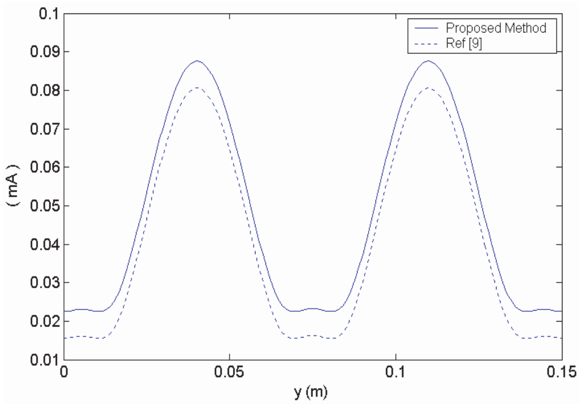

(b)

Figure 8. (a) Voltage magnitude and (b) current magnitude induced along the microstrip line ($\varphi_i = 90^\circ,\ \theta_i = 0$) at $f = 3\,\text{GHz}$.

the cross-section ($y = 0$) of a non-uniform microstrip line in Fig. 9 at $f = 3\,\text{GHz}$.

Selection of the number of segments and the width of the gap for a non-uniform microstip line depends on the type of transverse discontinuity and the desired precision. In Fig. 9(a), the current distribution in the cross-section of the microstrip line with a narrow transverse slit is shown for $s = 0.05W/M$ with the M as a parameter. It is seen that the effect of the number of the strips on the current distribution in the cross-section of this structure can be ignored for $M > 50$. Also, the effect of the width of the gap on the current distribution is depicted in Fig. 9(b) for $M = 50$.

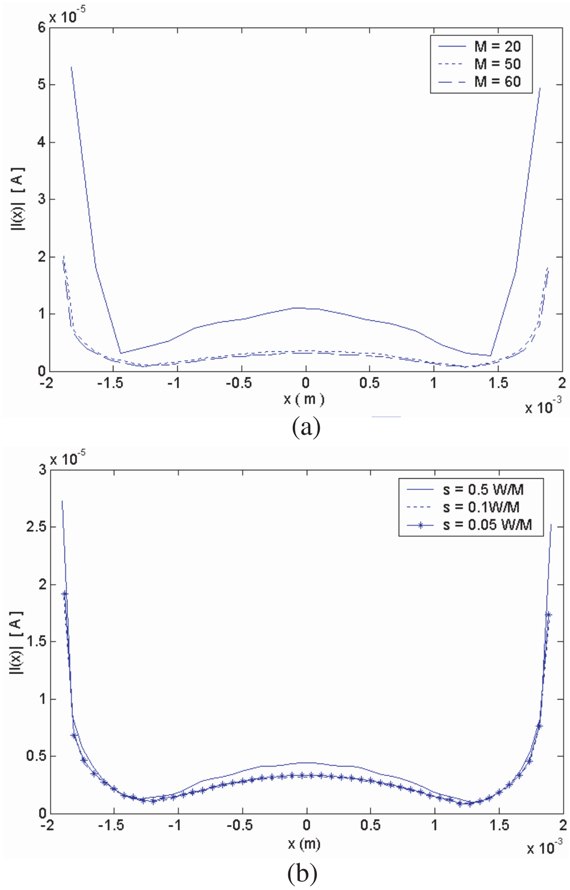

Figure 9. (a) The effect of the number of strips ($s = 0.05W/M$) and (b) the effect of the width of the gap ($M = 50$) on the current distribution in the cross-section ($y = 0$) of the non-uniform microstrip line at $f = 3\,\mathrm{GHz}$ ($\varphi_i = 90°,\ \theta_i = 45°$).

Consequently, if the conditions of $M > 50$ and $s < 0.05W/M$ are met simultaneously, the error caused by segmentation of a wide strip into multi-conductor strips will be negligible.

For the second structure, the induced voltage on the source and load terminals versus frequency is shown in change to Figs. 10 and 11 for $\varphi_i = 90°$, $\theta_i = 45°$, respectively. In both figures, it is observed that there is a good agreement between the results obtained using the RCMS method and HFSS. The execution time of the proposed method, using MATLAB software, on a desktop computer with Pentium-4 processor and 512 MB RAM, is about 8 minutes while the running time of the HFSS is approximately 2 hours and 18 minutes. It is obvious that this method is very efficient in terms of the running time and the computation load.

In Fig. 12, the induced voltage and current along the line are shown for different incidence angles in the y-z plane. For $\theta_i = 0$, the amplitude of the induced voltage and current is symmetric with respect to the center of line. The magnitude of the induced voltage for $\theta_i = 45°$ is greater than in the other cases (4.6 versus 4.1 and 3.6 mV). Also, the magnitude of the induced voltage is greater than in the first structure.

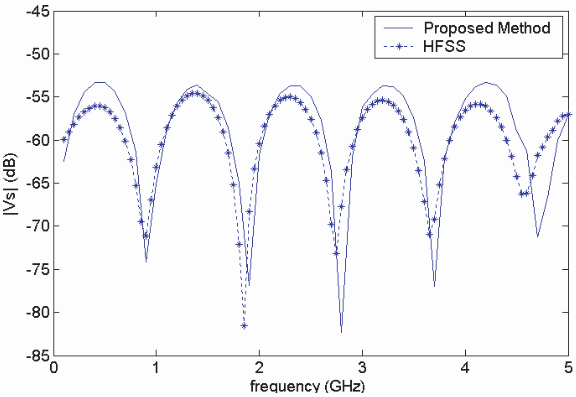

Figure 10. Induced voltage on the source terminal versus frequency for $\varphi_i = 90°$, $\theta_i = 45°$.

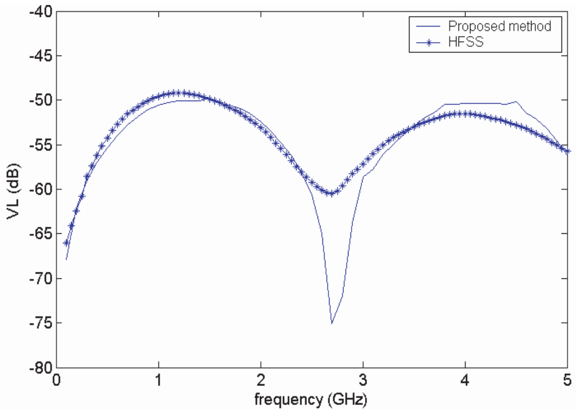

Figure 11. Induced voltage on the load versus frequency for $\varphi_i = 90°$, $\theta_i = 45°$.

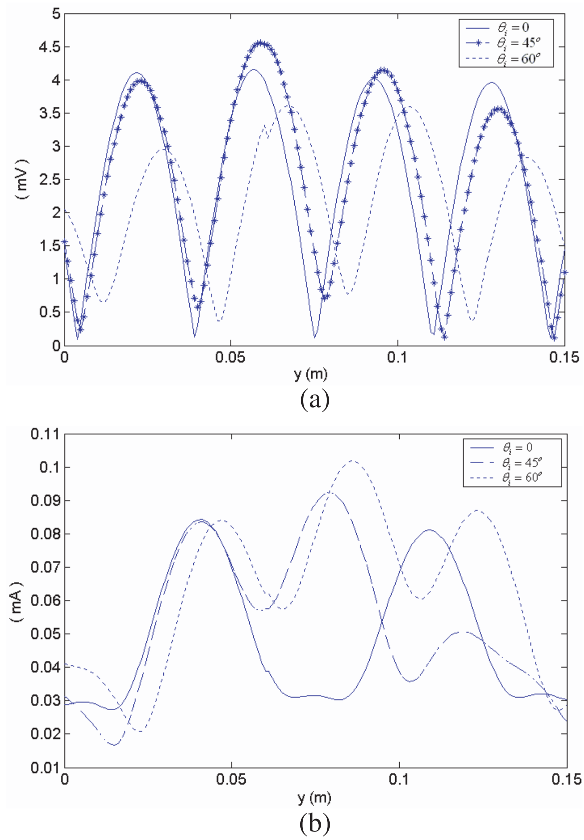

Figure 12. (a) Voltage magnitude and (b) current magnitude induced along the microstrip line with slit ($\varphi_i = 90°$) at $f = 3\,\mathrm{GHz}$.

7. CONCLUSION

The RCMS model and its capacitance and inductance matrices are introduced for the two-dimensional analysis of microstrip lines. This model is much simpler and faster than full wave analysis and can be used for structures with some non-uniformity in their width. This model has been used to find induced voltage and current along microstrip lines that have or do not have non-uniformity in the width of their strips and are illuminated by a uniform plane wave. The effect of incident angle on induced voltage and current has been investigated. We have compared the results with previous work and full wave results. The effectiveness of this approach to solve the microstrip structures that contain non-uniformity in their width has been shown.

REFERENCES

1. Collin, R. E., *Foundations of Microwave Engineering*, McGraw-Hill, 1992.
2. Pozar, D. M., *Microwave Engineering*, Addison Wesley, 1990.
3. Laroussi, R. and G. I. Costache, "Finite-element method applied to EMC problems [PCB environment]," *IEEE Trans. Electromagnetic Compatibility*, 178–184, May 1993.
4. Dhaene, T., L. Martens, and D. De Zutter, "Transient simulation of arbitrary nonuniform interconnection structures characterized by scattering parameters," *IEEE Trans. Circuits Systems-I: Fundamental Theory and Appl.*, 928–937, Nov. 1992.
5. Paul, C. R., *Analysis of Multi-conductor Transmission Lines*, John Wiley and Sons Inc., 1994.
6. Homentcovschi, D. and R. Oprea, "Analytically determined quasi-static parameters of shielded or open multi-conductor microstrip lines," *IEEE Trans. Microwave Theory Tech.*, 18–24, Jan. 1998.
7. Cheldavi, A. and A. M. Khalaj, "A new two dimensional analysis of microstrip lines using rigorously coupled multiconductor strips model," *Journal of Electromagnetic Waves and Applications*, Vol. 18, No. 6, 809–825, 2004.
8. Lei, G. T., G. W. Pan, and B. K. Gilbert, "Examination, clarification, and simplification of modal decoupling method for multiconductor transmission lines," *IEEE Trans. Microwave Theory Tech.*, Vol. 43, No. 9, 2090–2099, Sep. 1995.
9. Bernardi, P. and R. Cicchetti, "Response of a planar microstrip line excited by an external electromagnetic field," *IEEE Trans. Electromagnetic Compatibility*, Vol. 32, No. 2, 98–105, Jan. 1990.
10. Hoefer, W. J. R., "Equivalent series inductivity of a narrow transverse slit in microstrip," *IEEE Trans. Microwave Theory Tech.*, Vol. 25, No. 10, 822–824, Oct. 1977.
11. Khodabakhshi, H. and A. Cheldavi, "EM field coupling to microstrip lines using rigorously coupled multi-conductors strips," *APEMC 2008*, 874–877, Singapore, May 2008.